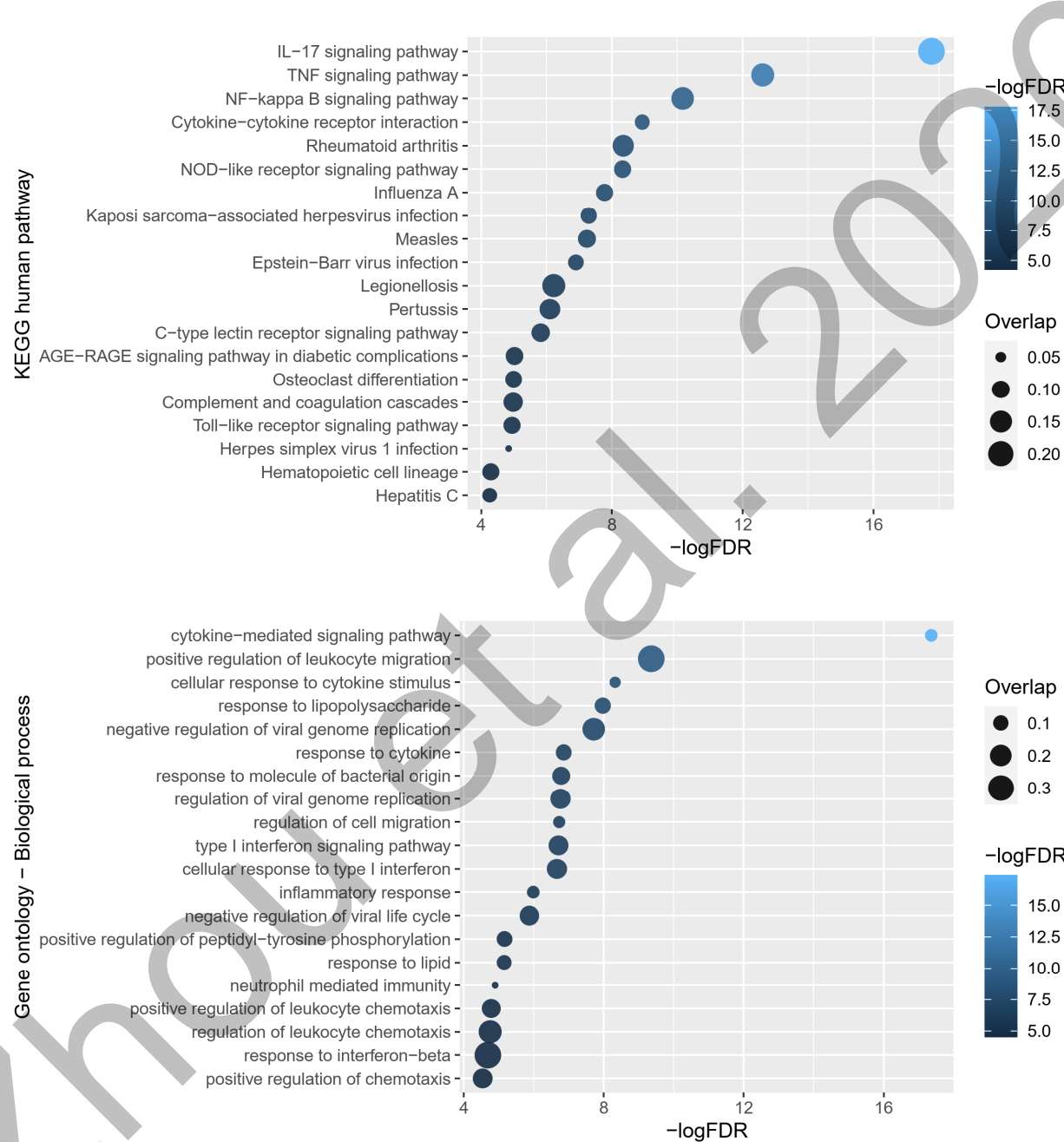


S1 Fig

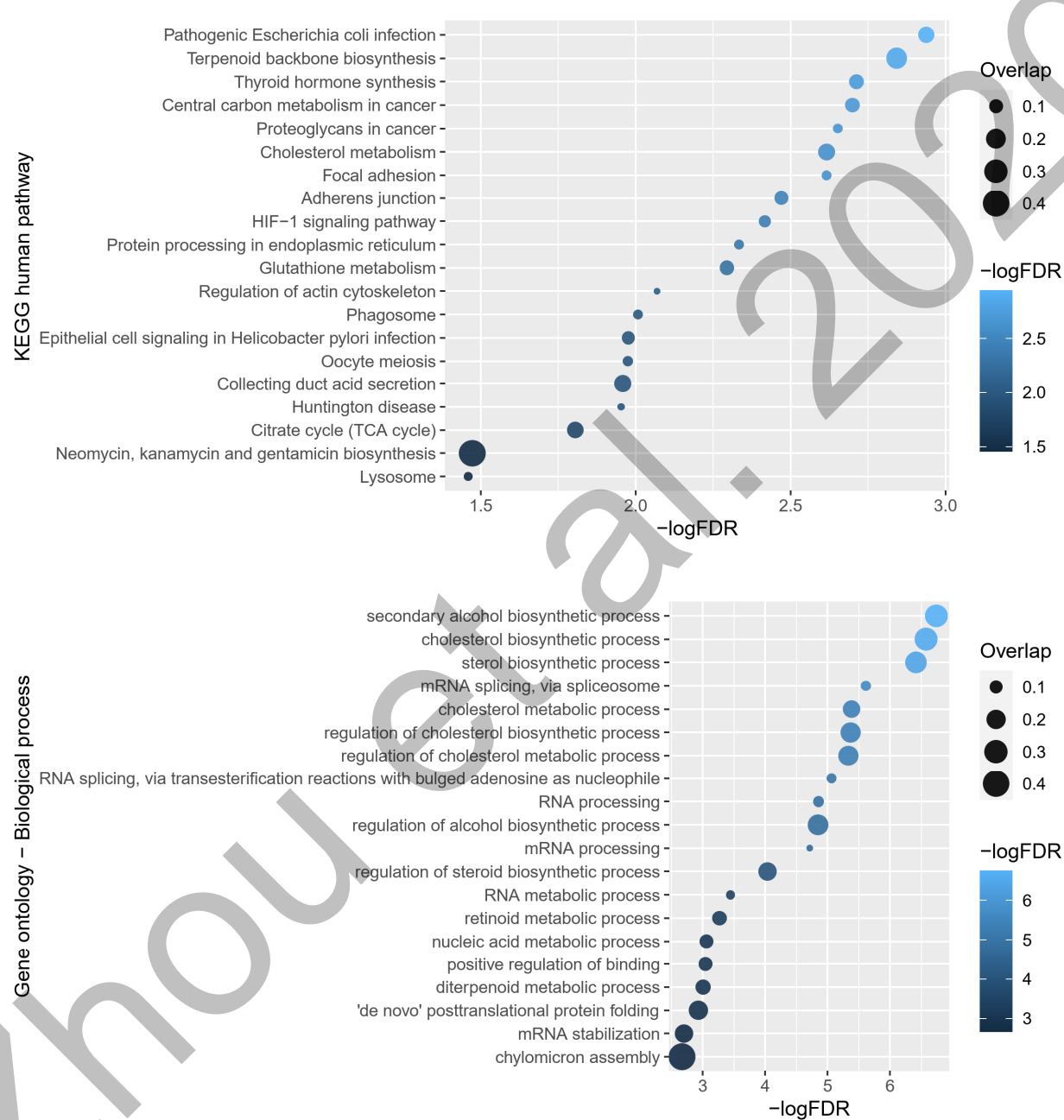
SARS2-DEG



S1 Fig. Functional enrichment analysis for SARS2-DEG. 246 differentially expressed genes (DEGs) in human bronchial epithelial cells infected with SARS-CoV-2 were obtained from the NCBI GEO database with the accession number GSE147507, denoted as SARS2-DEG.

S2 Fig

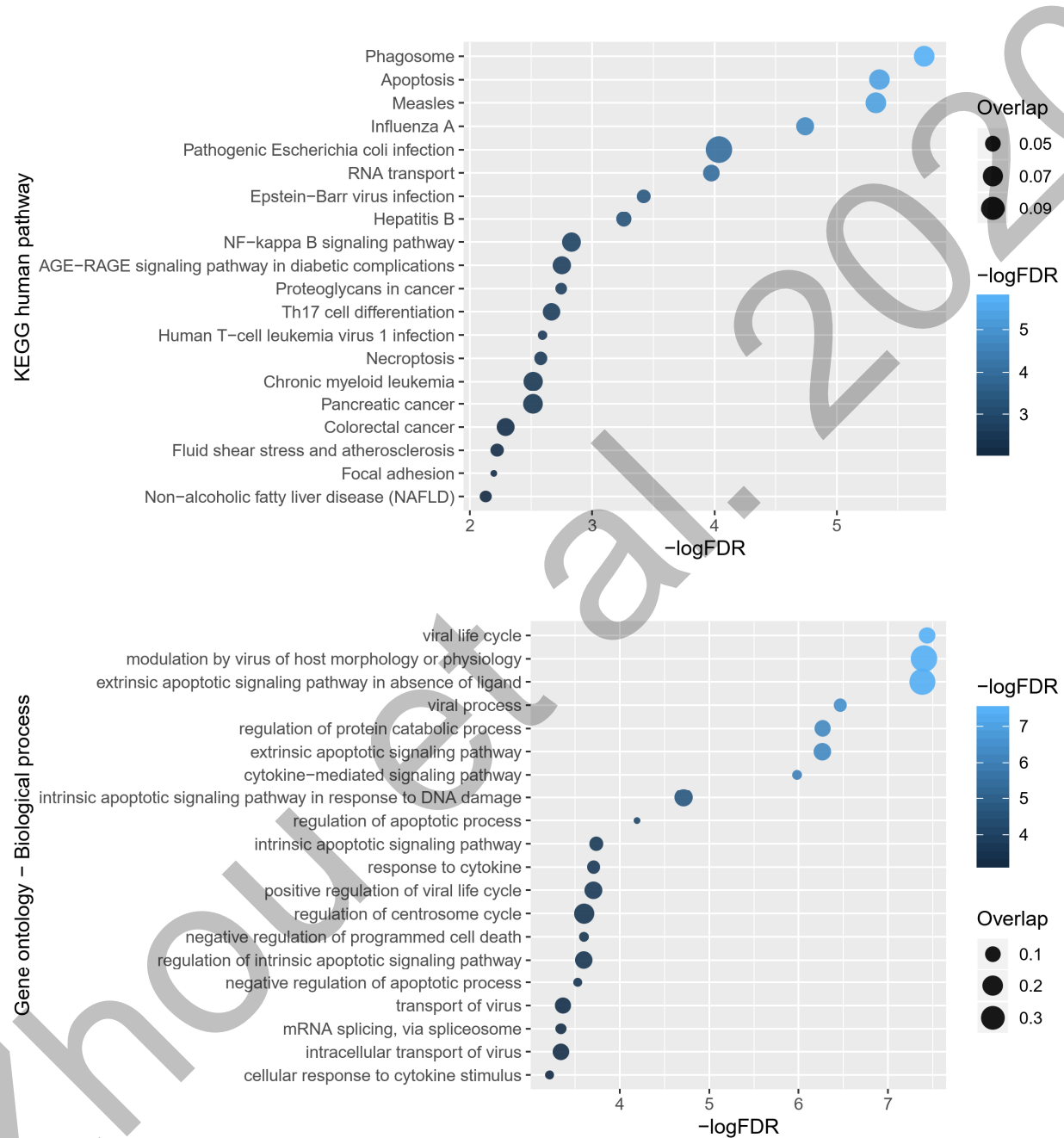
SARS2-DEP



S2 Fig. Functional enrichment analysis for SARS2-DEP. 293 differentially expressed proteins (DEPs) in human Caco-2 cells infected with SARS-CoV-2 were obtained from Bojkova, D. et al. (doi:10.1038/s41586-020-2332-7), denoted as SARS2-DEP.

S3 Fig

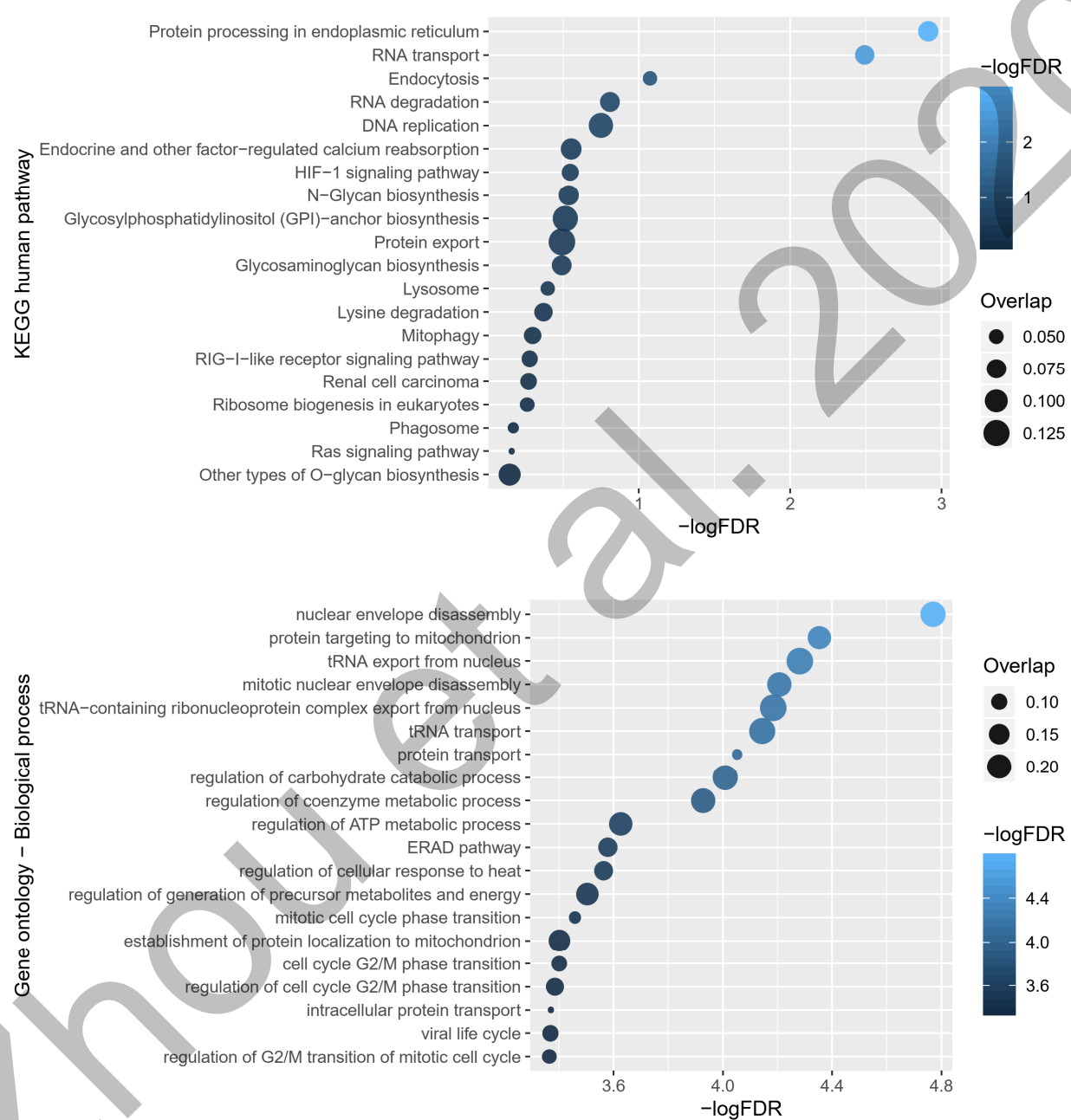
HCoV-PPI



S3 Fig. Functional enrichment analysis for HCoV-PPI. This data set contains 134 strong literature evidence-based pan-human coronavirus target host proteins from Zhou, Y. *et al.* (doi:10.1038/s41421-020-0153-3) with 15 newly curated proteins, denoted as HCoV-PPI.

S4 Fig

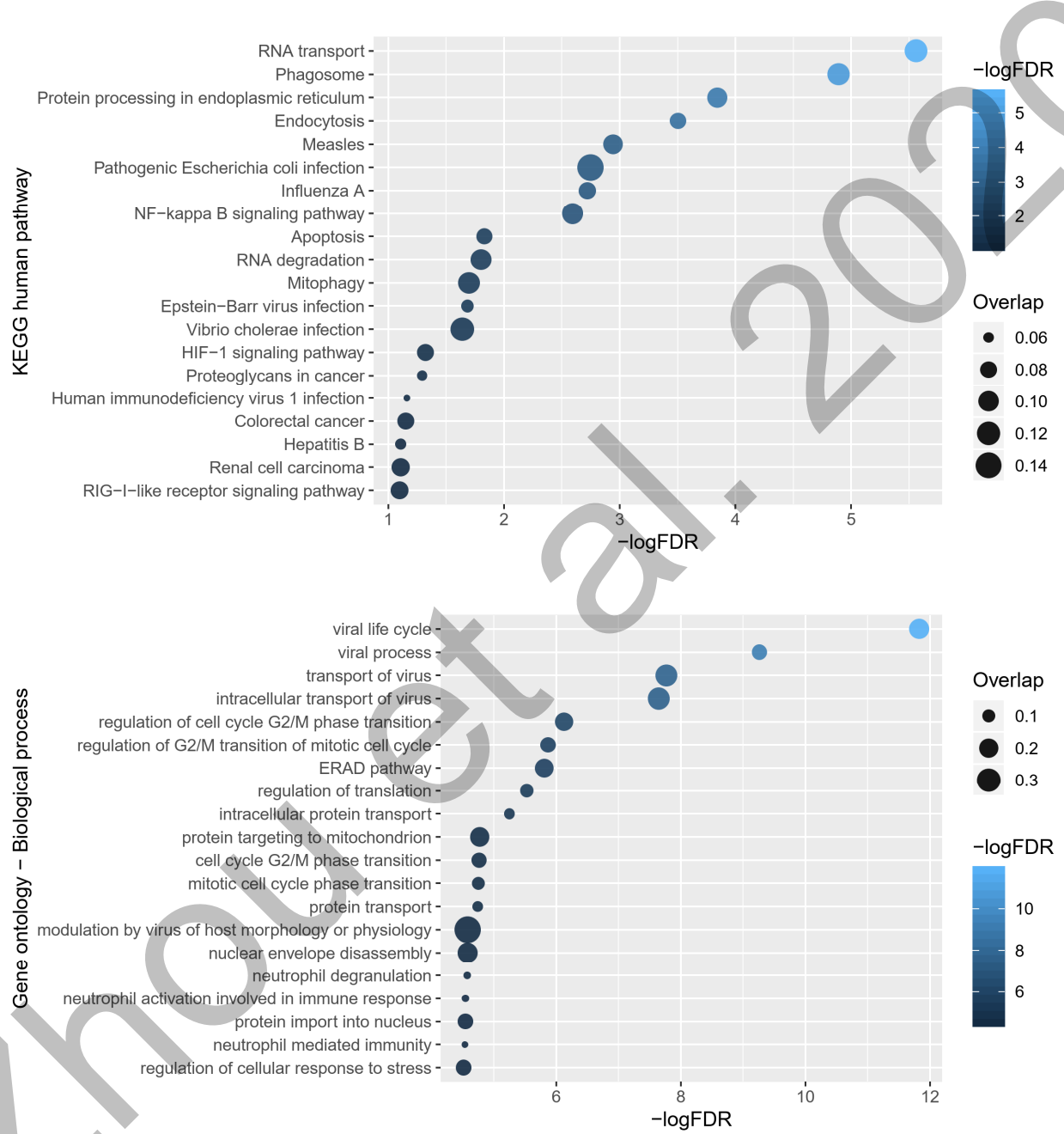
SARS2-PPI



S4 Fig. Functional enrichment analysis for SARS2-PPI. This data set contains 332 proteins involved in the protein-protein interactions with 26 SARS-CoV-2 viral proteins identified by affinity purification-mass spectrometry from Gordon, D. E. et al. (doi:10.1038/s41586-020-2286-9), denoted as SARS2-PPI.

S5 Fig

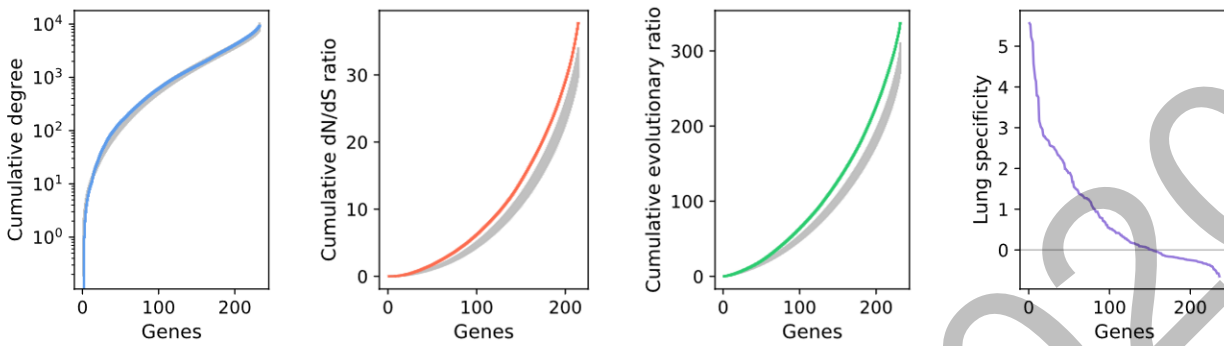
PanCoV-PPI



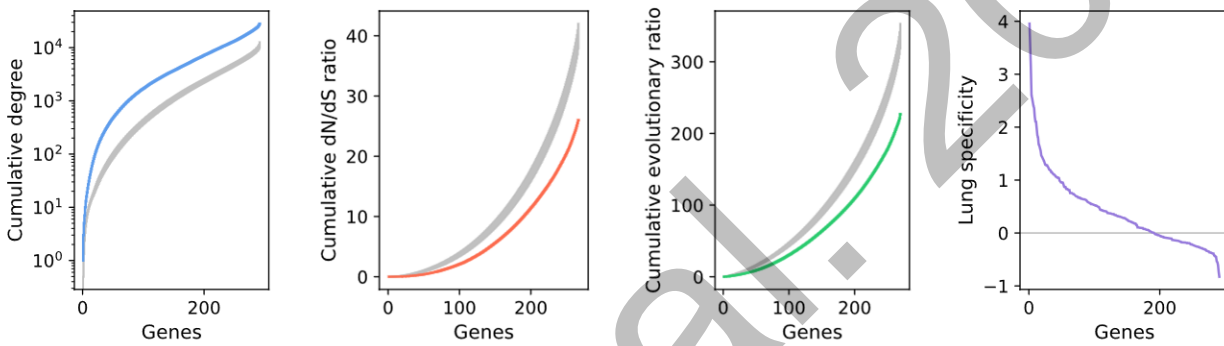
S5 Fig. Functional enrichment analysis for PanCoV-PPI. Due to the interactome nature of HCoV-PPI and SARS2-PPI, we combined these data sets as the fifth SARS-CoV-2 data set, which has 460 proteins and is denoted as PanCoV-PPI.

S6 Fig

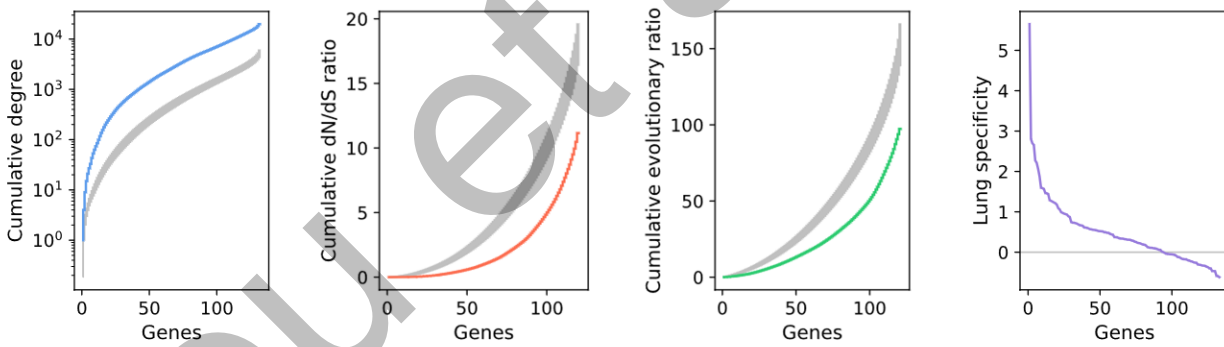
SARS2-DEG



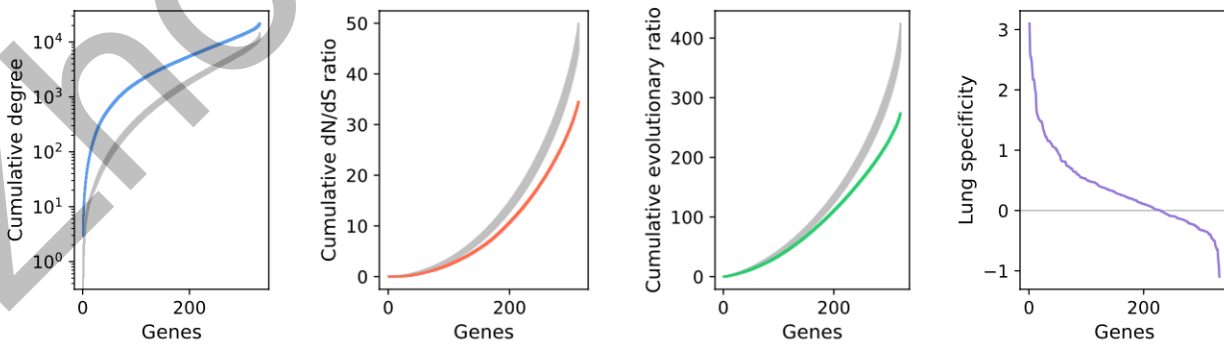
SARS2-DEP



HCoV-PPI

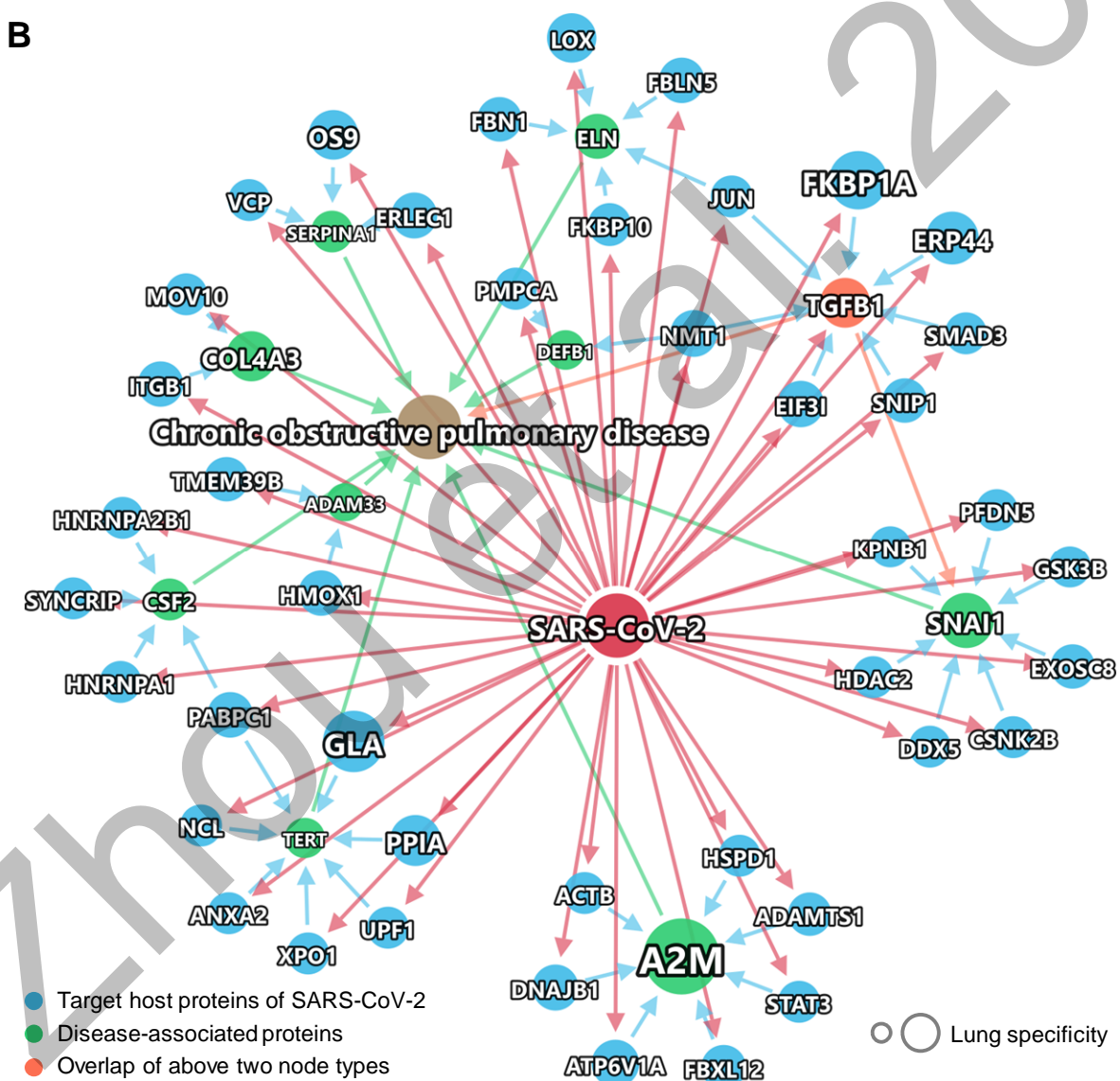
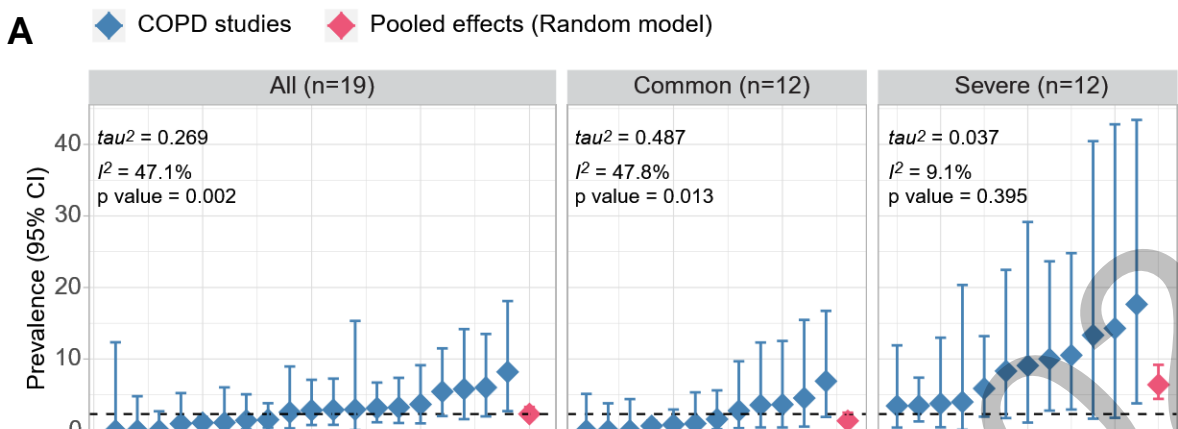


SARS2-PPI



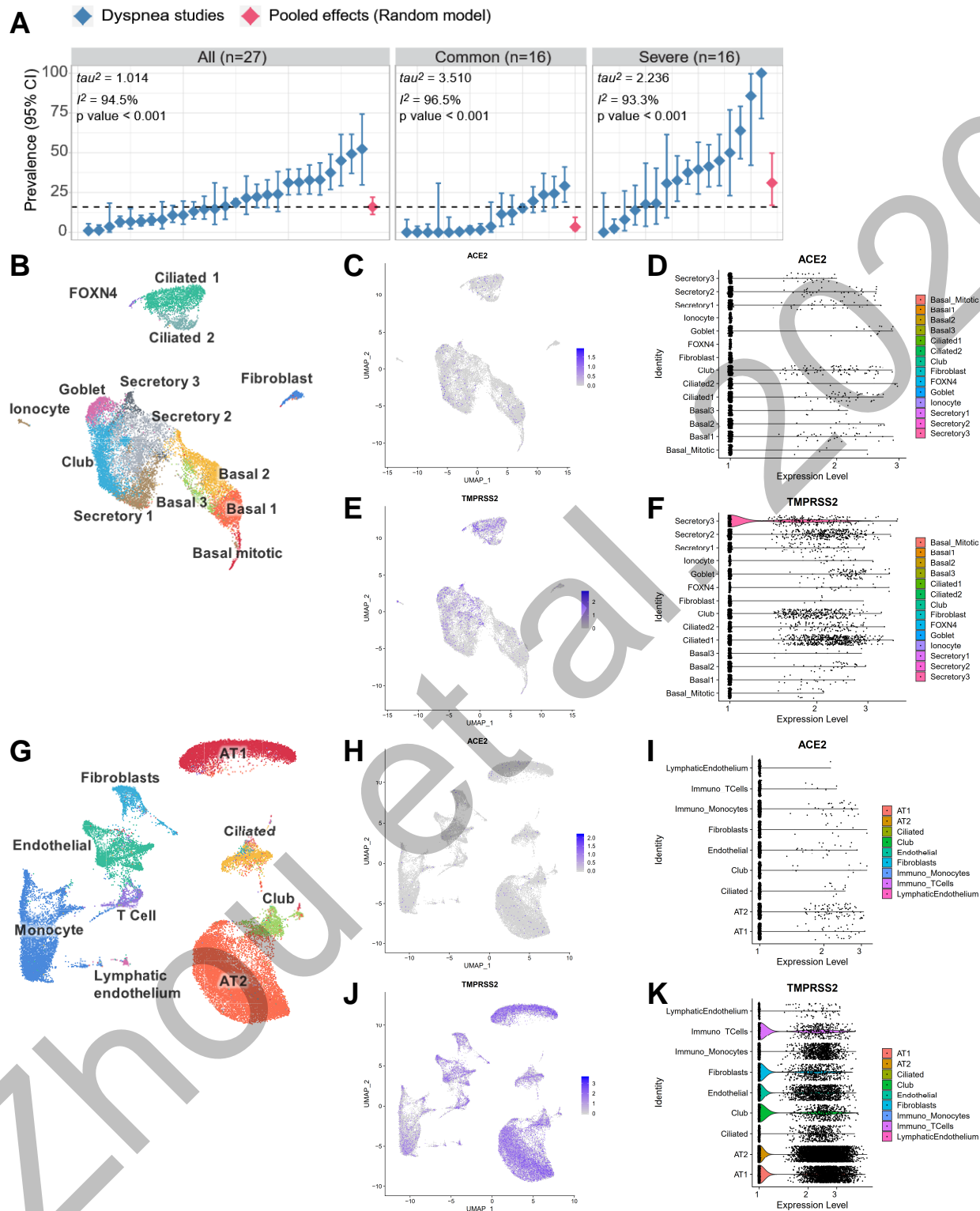
S6 Fig. Characteristics of the four SARS-CoV-2 target data sets. Node degree (blue), dN/dS ratio (orange), evolutionary ratio (green), and lung expression specificity (purple) are shown for each data sets. Grey areas indicate mean \pm standard deviation of 100 repeats using randomly selected genes.

S7 Fig



S7 Fig. Chronic obstructive pulmonary disease and COVID-19. (A) The risk of chronic obstructive pulmonary disease (COPD) is increased in severe COVID-19 patients. (B) Subnetwork shows the proteins potentially involved in the interaction between COPD and COVID-19.

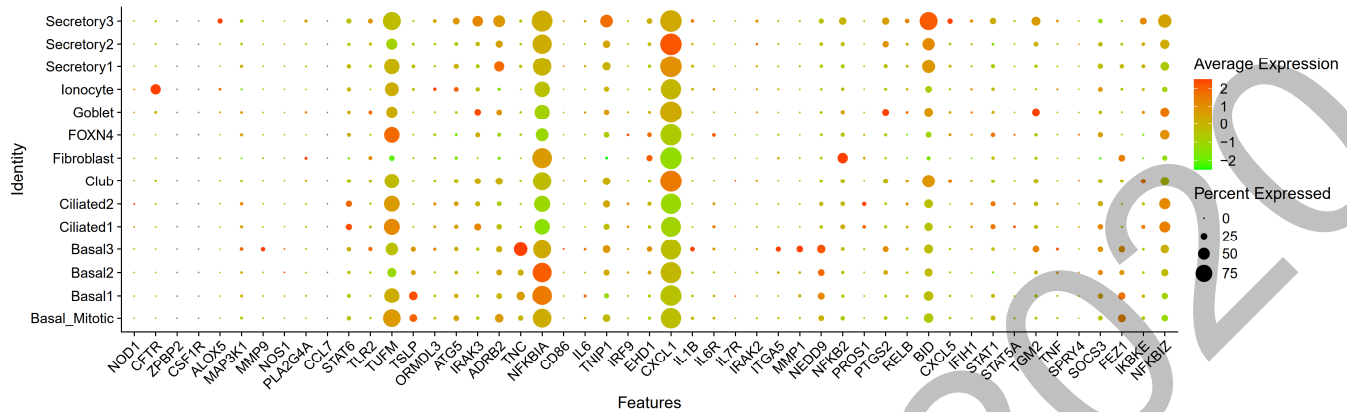
S8 Fig



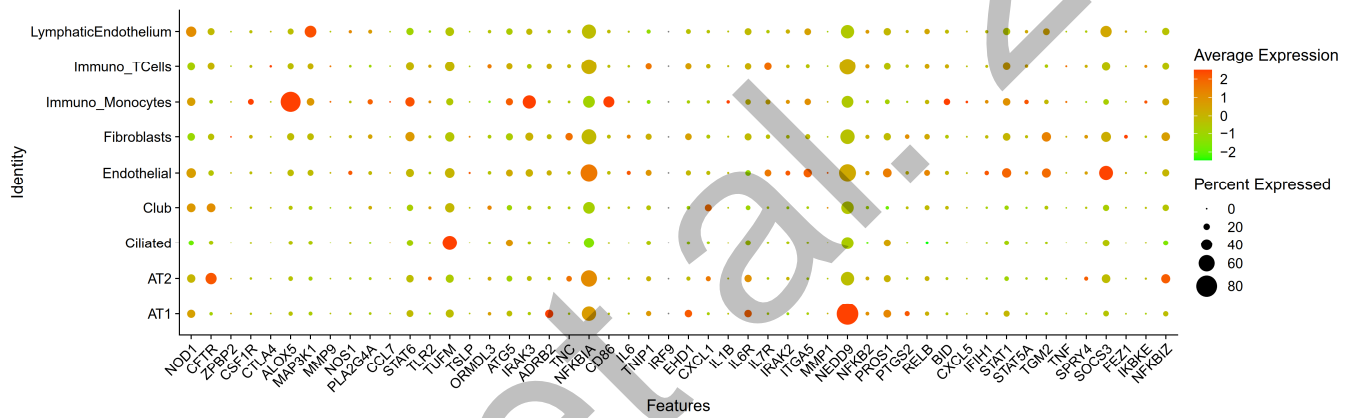
S8 Fig. Asthma and COVID-19. (A) The risk of dyspnea is increased in severe COVID-19 patients. (B) UMAP visualization for human bronchial epithelial cells. (C, D) Expression levels of ACE2 across 14 cell types. (E, F) Expression levels of TMPRSS2 across 14 cell types. (G) UMAP visualization for lung cells. (H, I) Expression levels of ACE2 across 9 cell types. (J, K) Expression levels of TMPRSS2 across 9 cell types. The single cell data with cell type annotation were retrieved from Lukassen, S. et al. (doi:10.15252/embj.20105114), which contains 39,778 lung cells and 17,451 bronchial epithelial cells.

S9 Fig

A

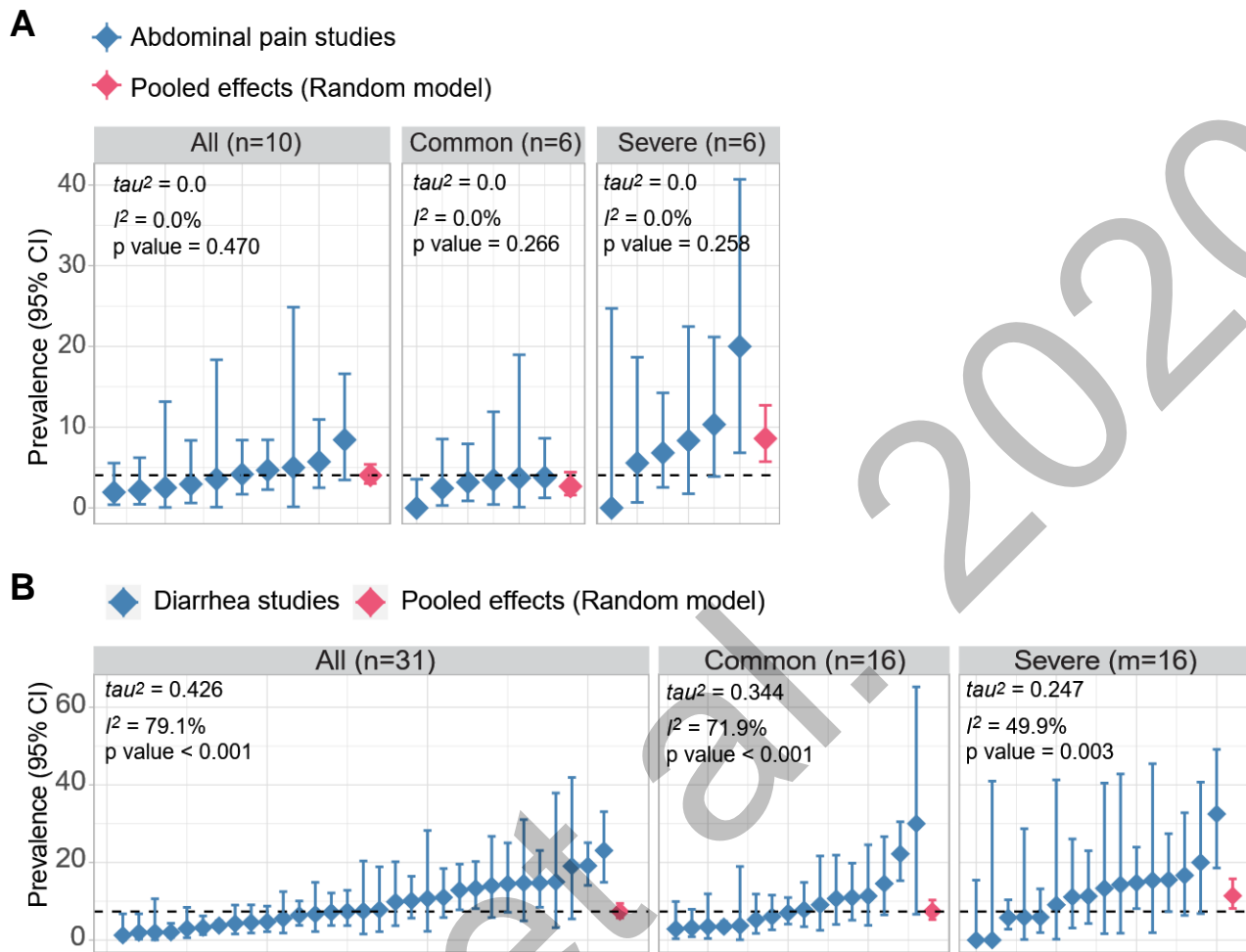


B



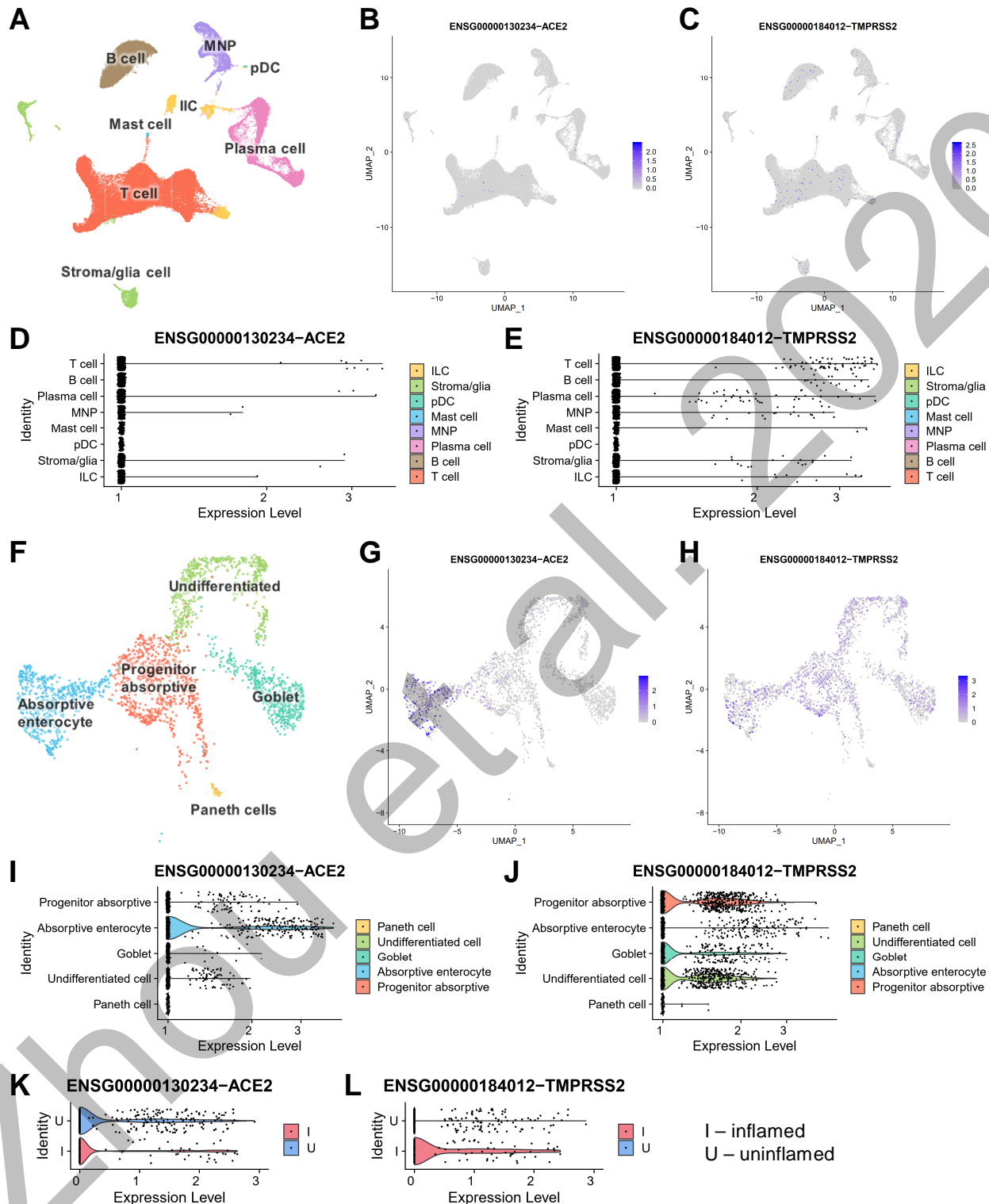
S9 Fig. The expression of asthma genes and SARS-CoV-2 targets. The expression levels of the genes from the asthma-COVID-19 subnetwork in bronchial epithelial cells (A) and lung cells (B) are shown.

S10 Fig



S10 Fig. Risk ratios for abdominal pain and diarrhea in COVID-19 patients. Abdominal pain (**A**) and diarrhea (**B**) have increased risks in severe COVID-19 patients.

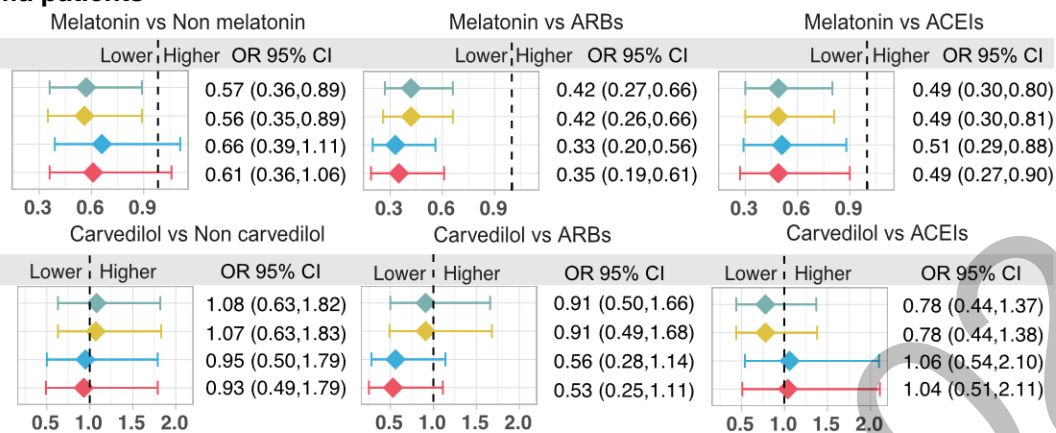
S11 Fig



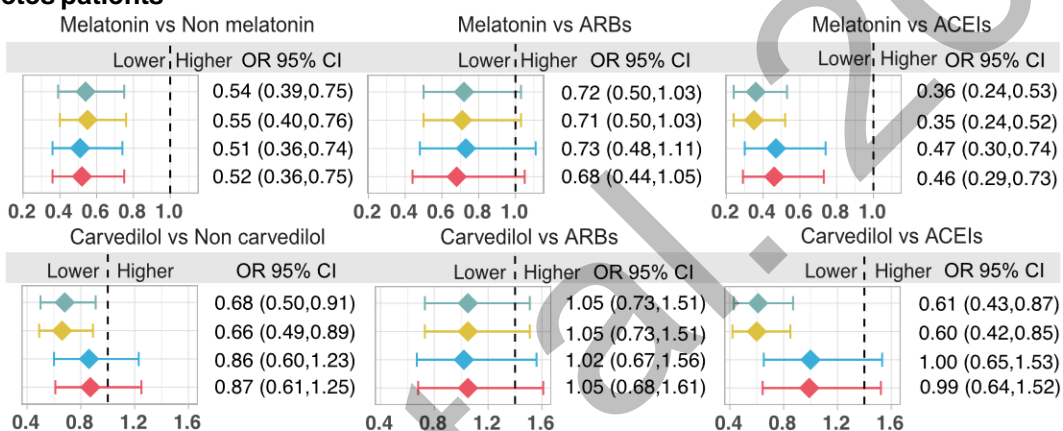
S11 Fig. Inflammatory bowel disease and COVID-19. (A) UMAP visualization of non-epithelial cells from the ileal tissues of patients with Crohn's disease. (B, D) The expression of ACE2 in non-epithelial cells in A. (C, E) The expression of TMPRSS2 in non-epithelial cells in A. (F) UMAP visualization of epithelial cells from the ileal tissues of patients with Crohn's disease. (G, I) The expression of ACE2 in epithelial cells in F. (H, J) The expression of TMPRSS2 in epithelial cells in F. (K, L) The expression levels of ACE2 and TMPRSS2 in the inflamed versus uninflamed ileal absorptive enterocytes in Crohn's disease patients. The single cell data were retrieved from Martin, J. C. et al. (doi:10.1016/j.cell.2019.08.008), which contains 67,050 inflamed and uninflamed cells from the ileal samples of 8 patients with Crohn's disease.

S12 Fig

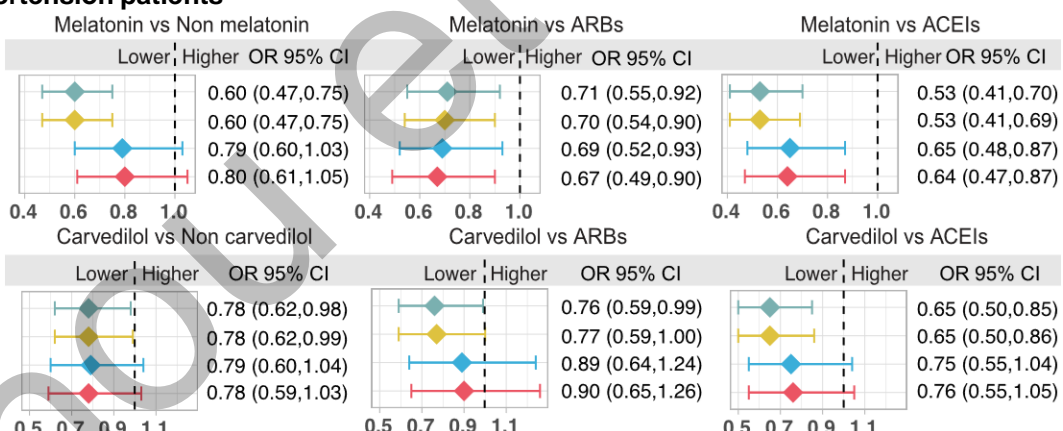
A. Asthma patients



B. Diabetes patients



C. Hypertension patients



Propensity score matching using

- ◆ age, gender, race, smoking
- ◆ age, gender, race, smoking
- ◆ age, gender, race, smoking, coronary artery disease, diabetes, hypertension, and COPD
- ◆ age, gender, race, smoking, coronary artery disease, diabetes, hypertension, and COPD

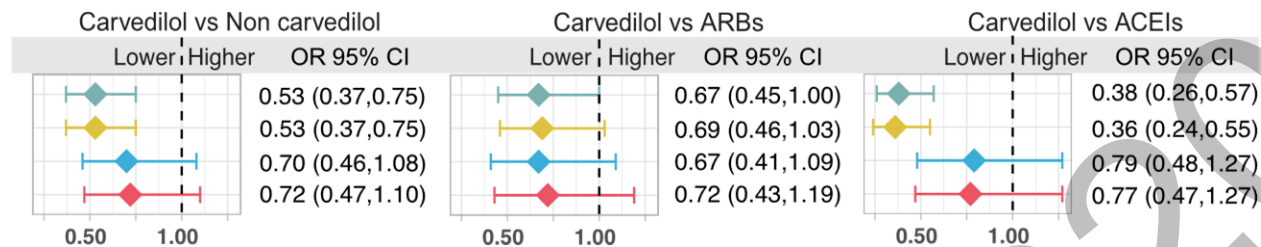
Odds ratios of COVID-19 adjusted by

- age, gender, race, smoking
- age, gender, race, smoking, coronary artery disease, diabetes, hypertension, and COPD

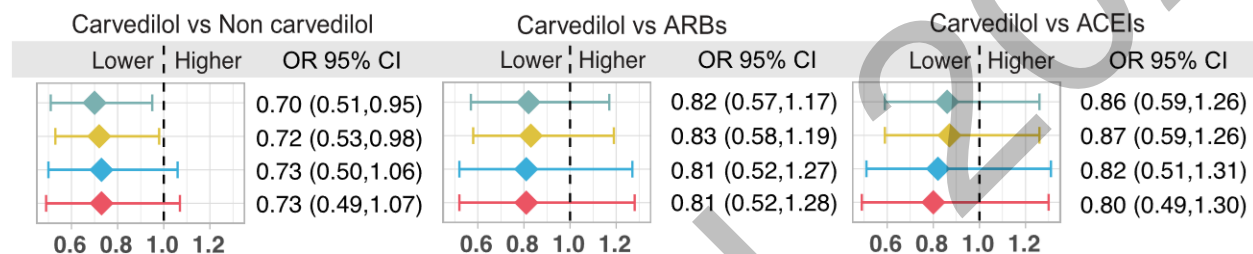
S12 Fig. Patient-based validation of drug repurposing for COVID-19 using three different subgroups, (A) asthma, (B) diabetes, and (C) hypertension. Four models were evaluated. These models were matched and adjusted using different variables as shown in the table. The variable that was used to extract each patient subgroup was not used for propensity score matching or odds ratios adjustment. ACEIs, angiotensin-converting enzyme inhibitors. ARBs, angiotensin II receptor blockers.

S13 Fig

A. Black Americans



B. White Americans



Propensity score matching using

- ◆ age, gender, smoking
- ◆ age, gender, smoking
- ◆ age, gender, smoking, coronary artery disease, diabetes, hypertension, and COPD
- ◆ age, gender, smoking, coronary artery disease, diabetes, hypertension, and COPD

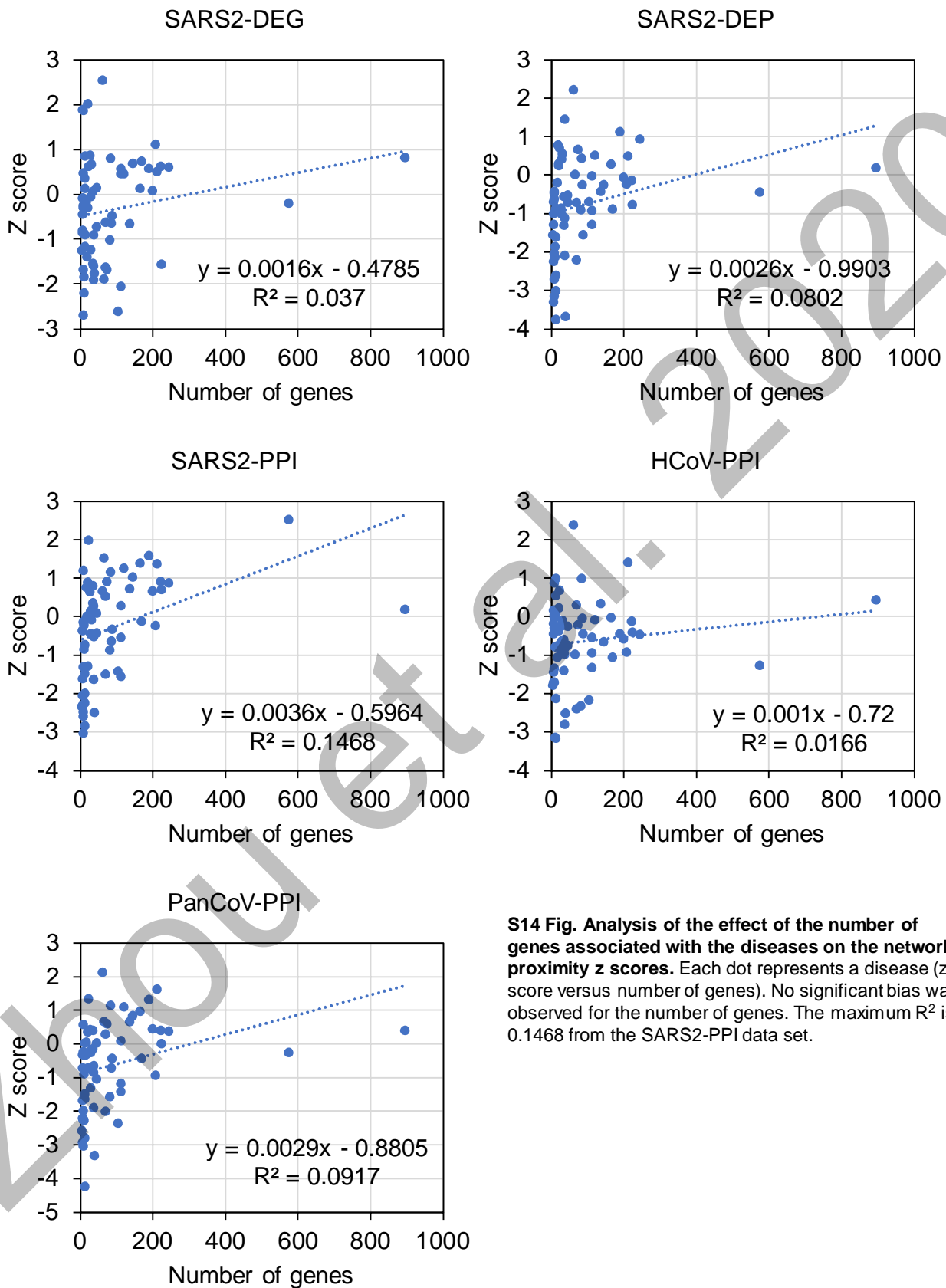
Odds ratios of COVID-19 adjusted by

age, gender, smoking

age, gender, smoking, coronary artery disease, diabetes, hypertension, and COPD

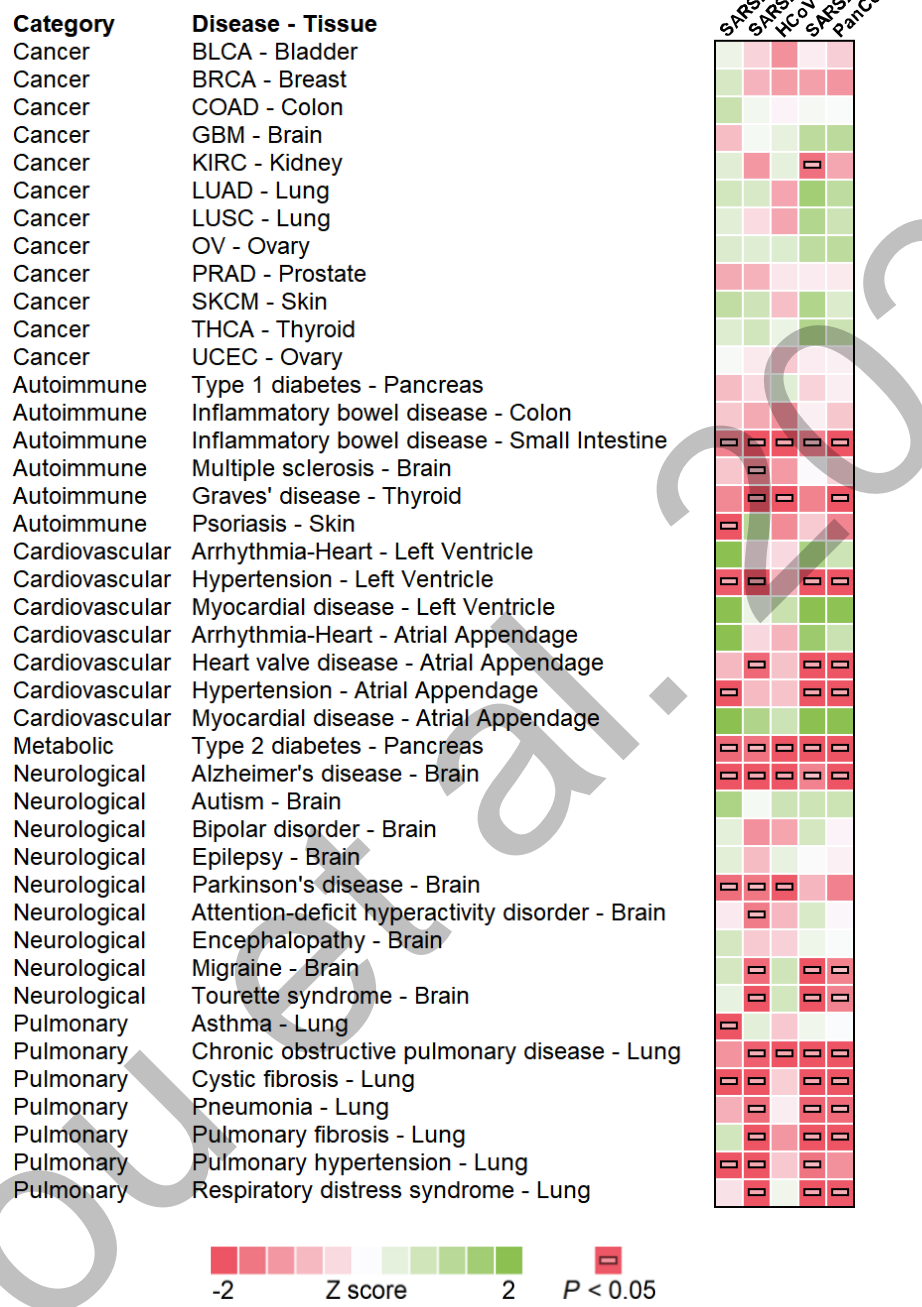
S13 Fig. Comparison of the patient validation results of carvedilol intake in black Americans and white Americans. In black Americans, carvedilol intake showed a lowered risk of a positive COVID-19 diagnosis when propensity score was matched with basic variables (age, gender, and smoking).

S14 Fig



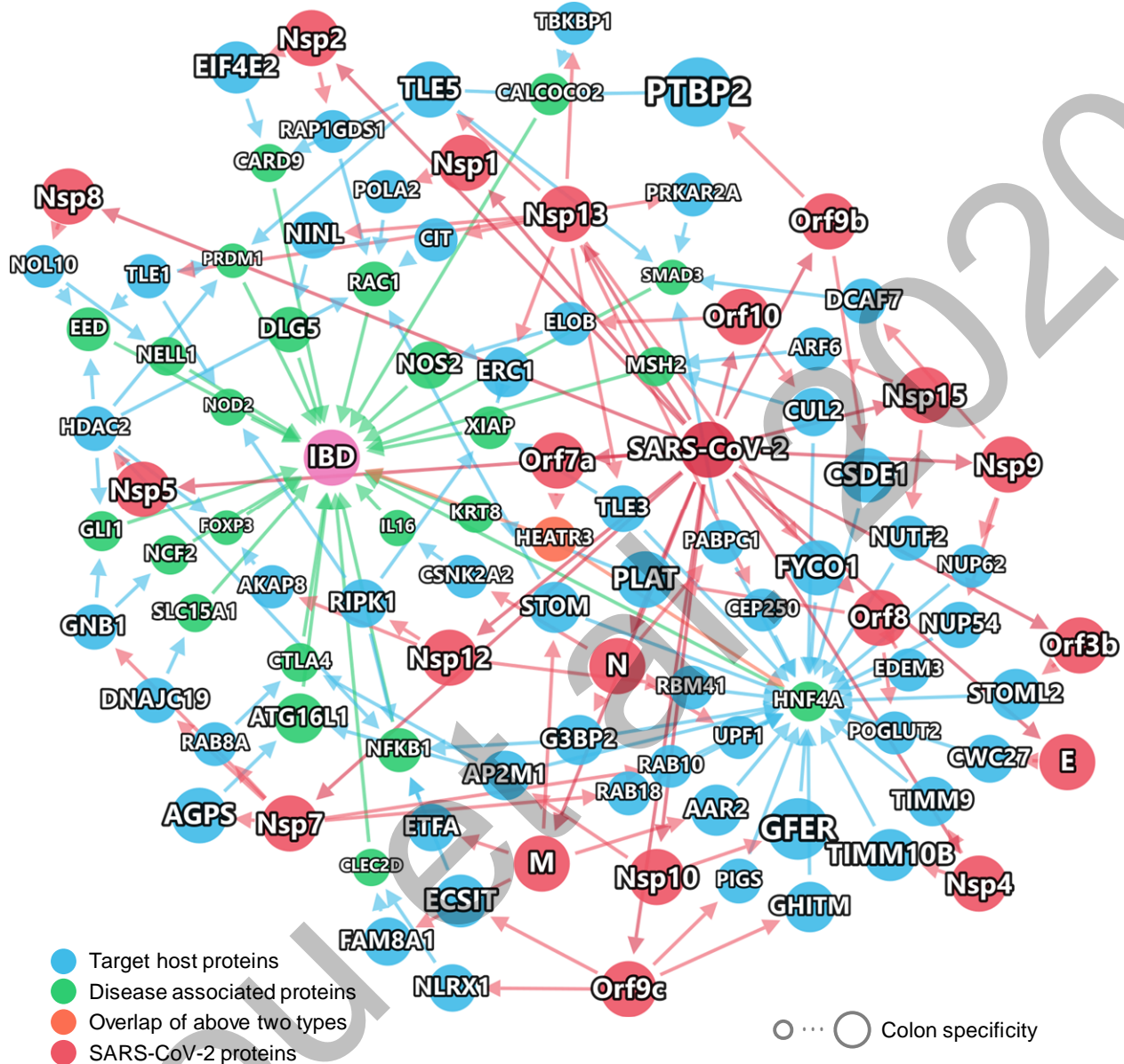
S14 Fig. Analysis of the effect of the number of genes associated with the diseases on the network proximity z scores. Each dot represents a disease (z score versus number of genes). No significant bias was observed for the number of genes. The maximum R^2 is 0.1468 from the SARS2-PPI data set.

S15 Fig



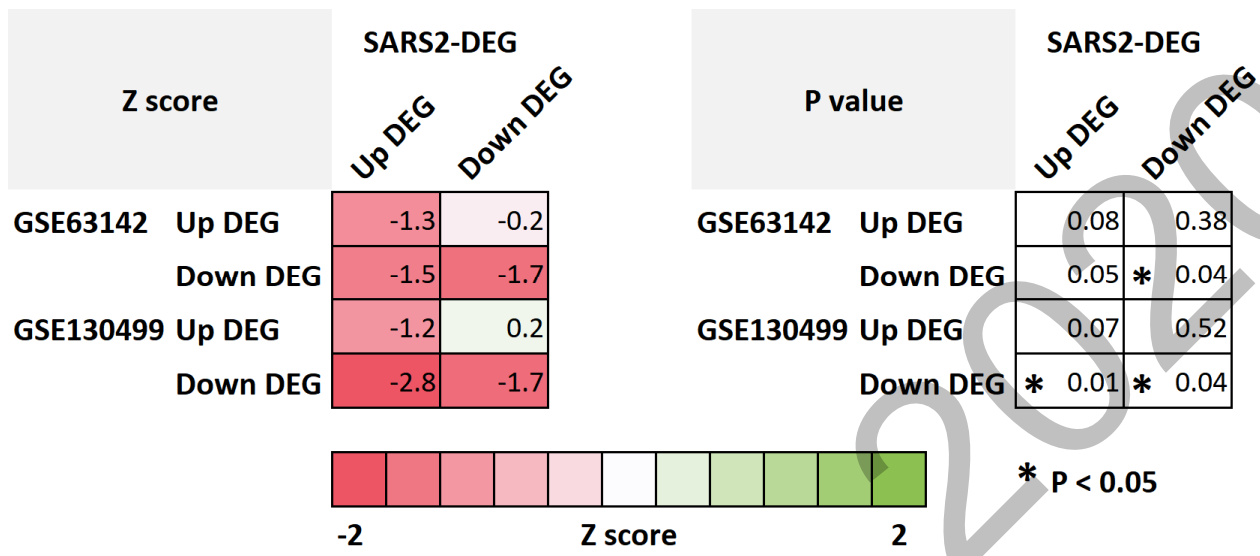
S15 Fig. Disease manifestations associated with COVID-19 quantified by network proximity measure using tissue-specific genes for each disease. The disease-associated genes were filtered by their tissue specificity. Tissues considered are shown after the disease names. Only genes with positive specificity were retained for the network analysis. After filtering, diseases with less than 5 genes were removed from the evaluation.

S16 Fig



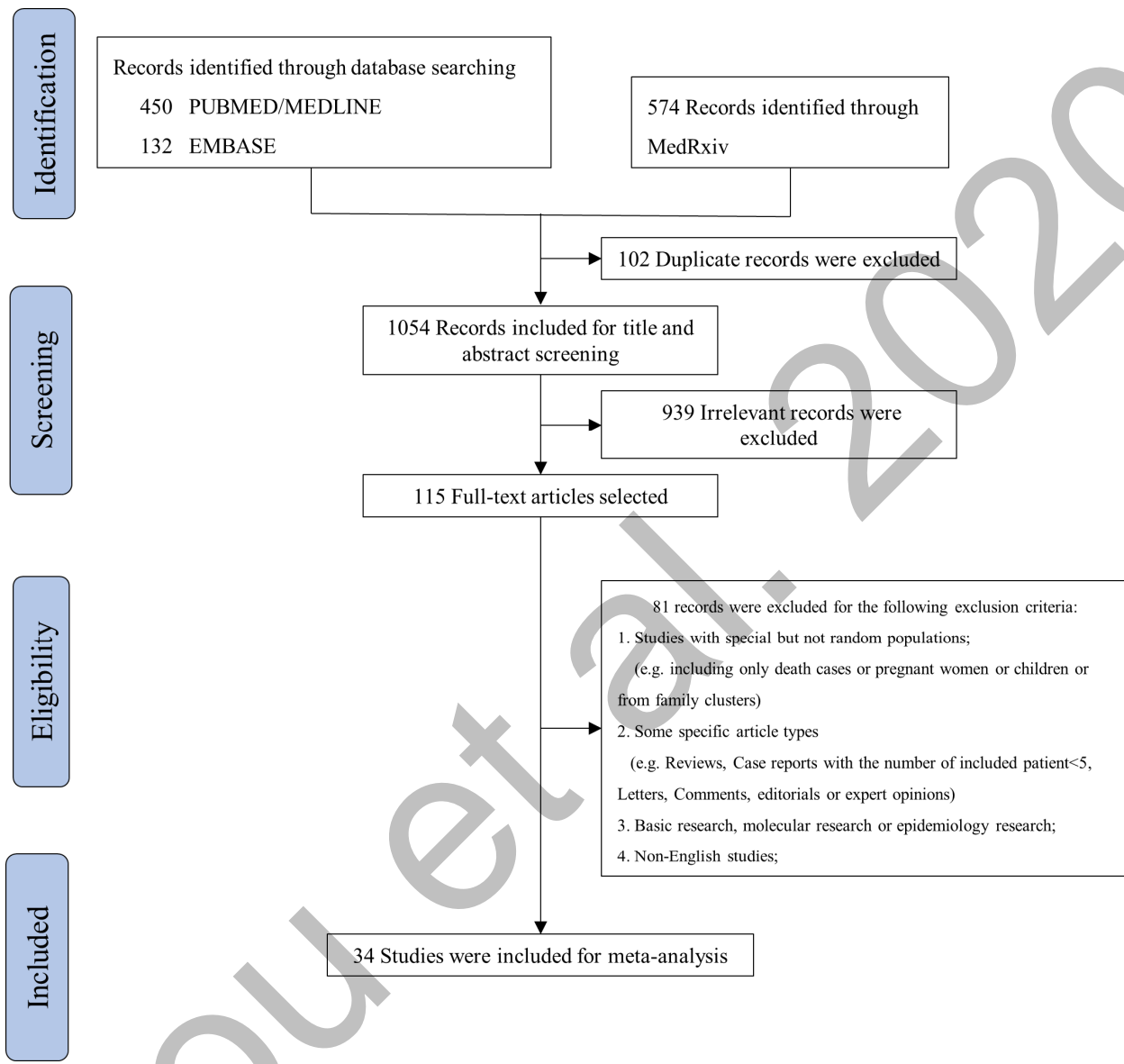
S16 Fig. The subnetwork between the IBD-associated genes, the SARS-CoV-2 virus proteins, and virus target proteins. Node sizes show their tissue specificity in colon.

S17 Fig



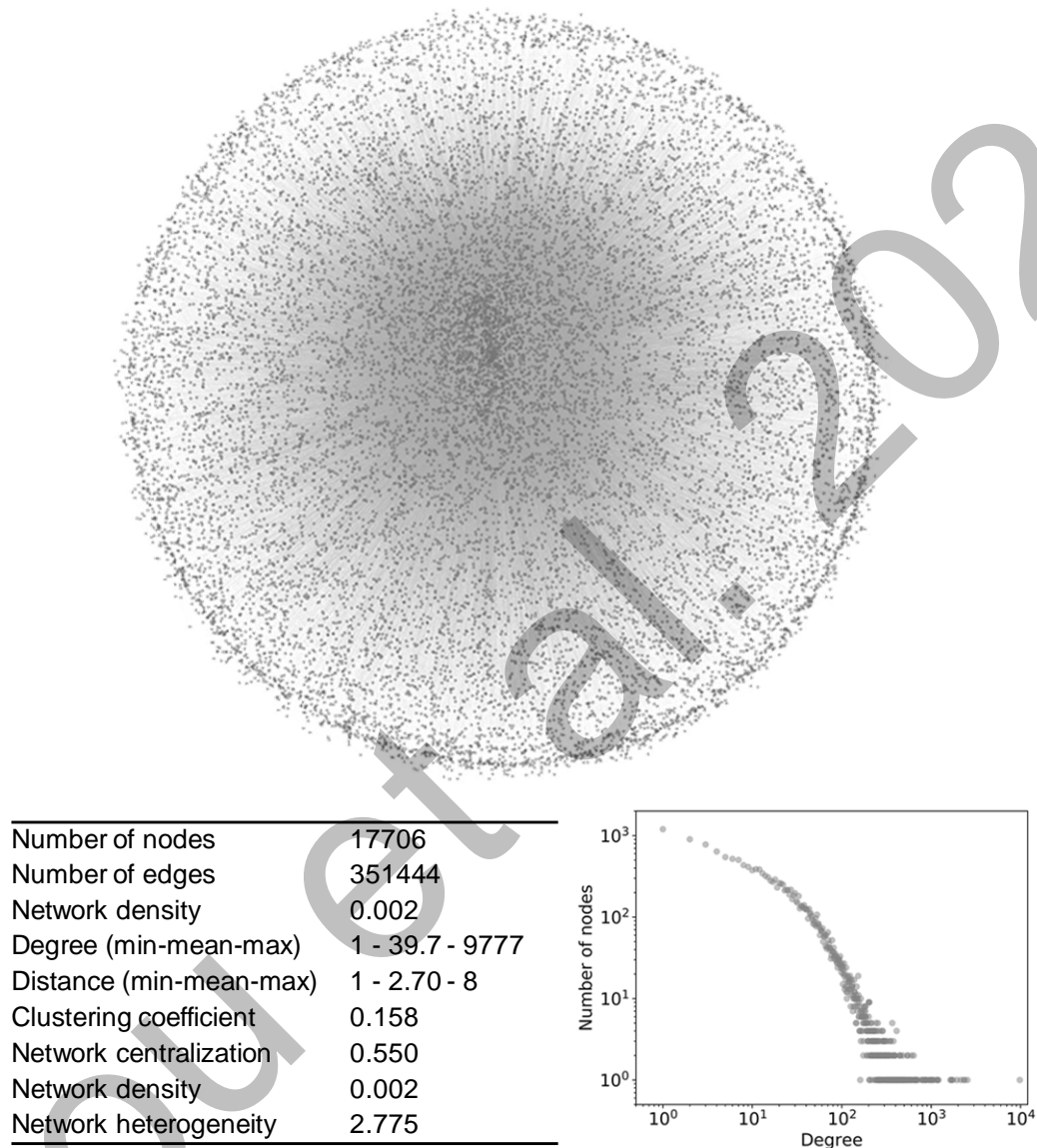
S17 Fig. Network proximity analysis of asthma and COVID-19 taking into consideration the directionalities of the differential gene expression. The up- and down- expressed genes in the two asthma data sets (GSE63142 and GSE130499, severe vs. control) were computed against the up- and down- expressed genes from the SARS2-DEG data set. Overall, the results show more significant network proximities and smaller z scores than when the direction is not considered as in Fig 4.

S18 Fig



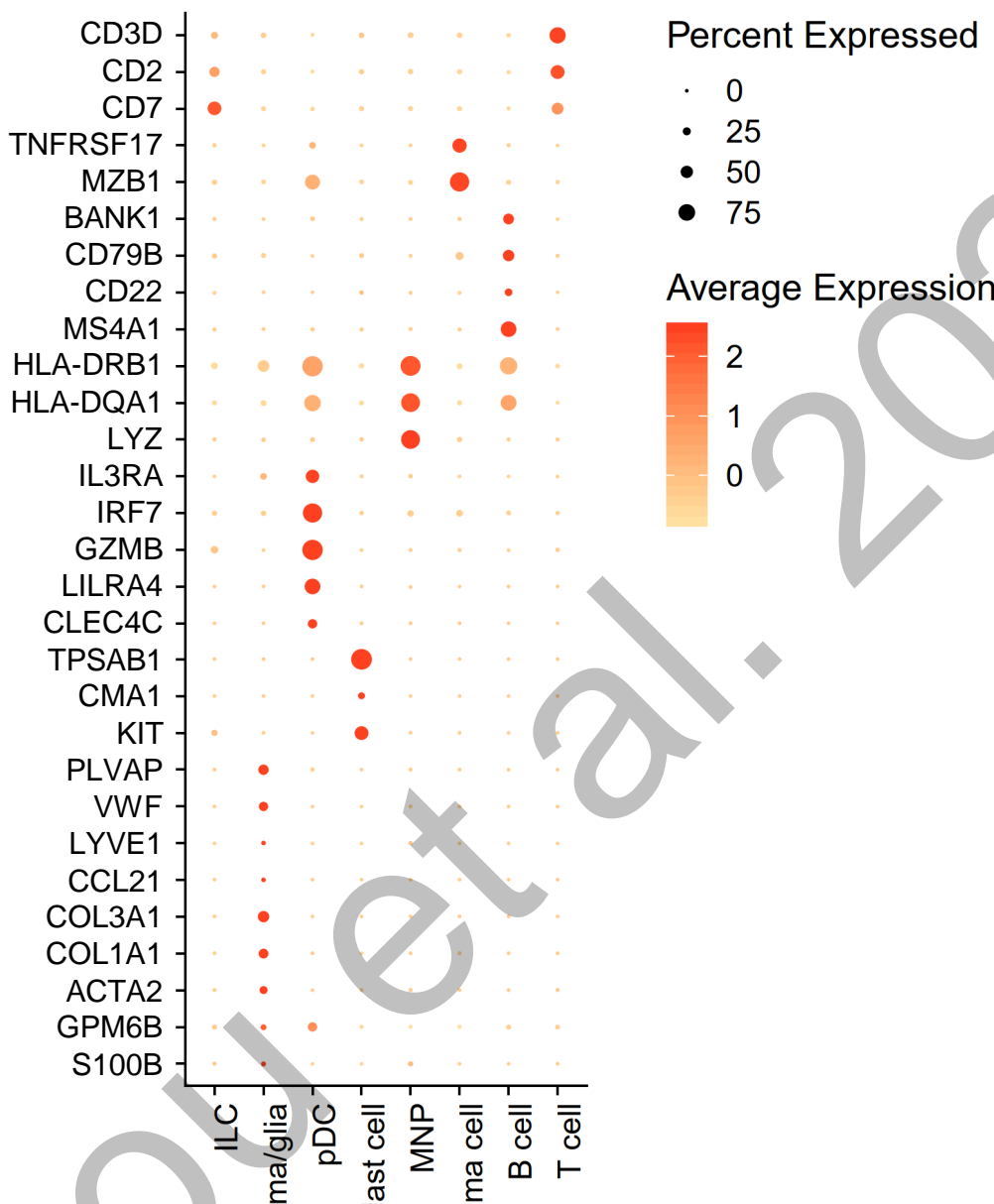
S18 Fig. Workflow of clinical study search. We searched PubMed, Embase, and Medrxiv databases for publications as of April 25th, 2020 using the search term (“SARS-COV-2” OR “COVID-19” OR “nCoV 19” OR “2019 novel coronavirus” OR “coronavirus disease 2019”) AND (“clinical characteristics” OR “clinical outcome” OR “comorbidities”). Only research articles were included. Several criteria were used to filter the initial 1,054 articles to a final of 34 studies for meta-analyses.

S19 Fig



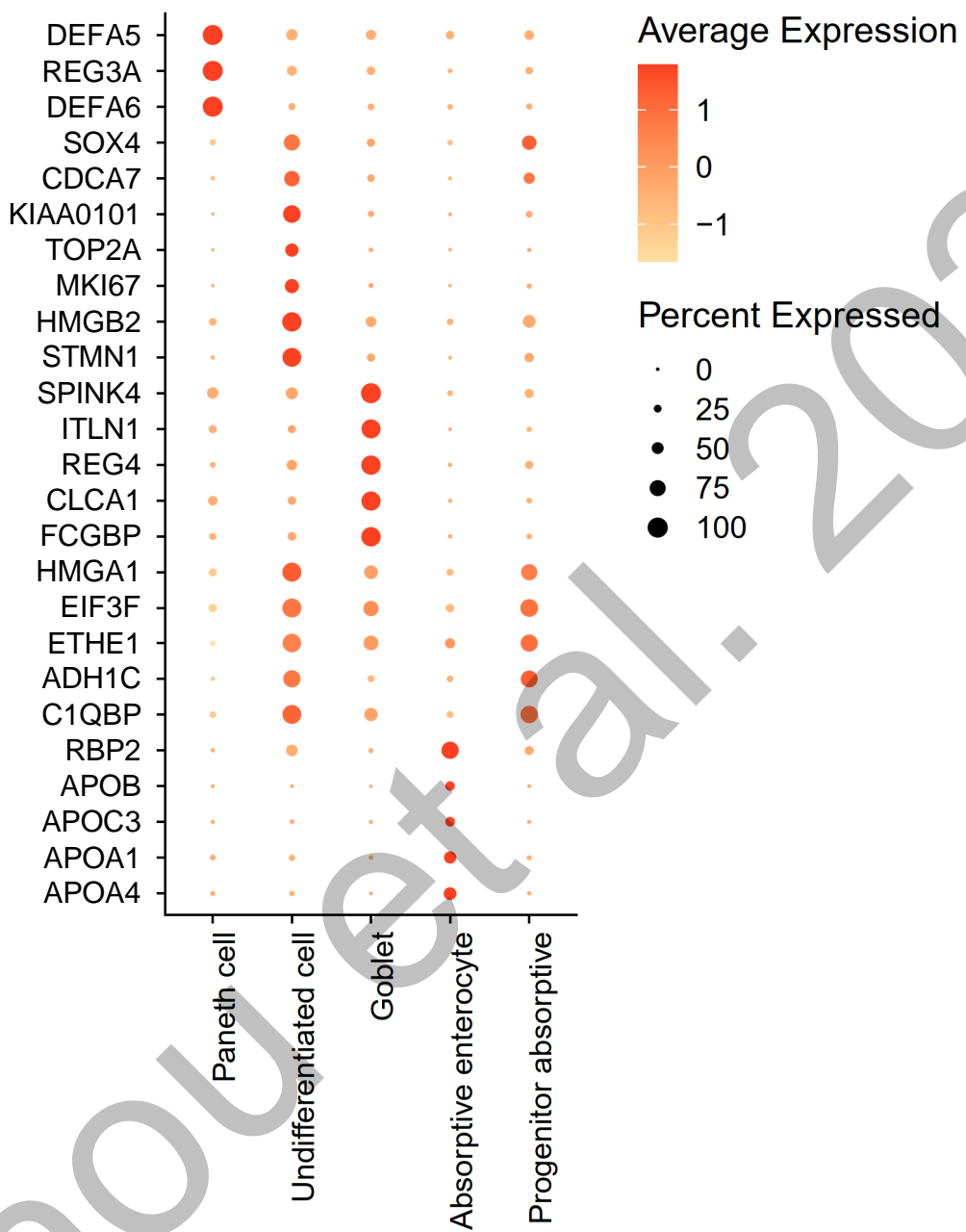
S19 Fig. Overview of the human protein interactome. Cytoscape 3.7.1 was used for the visualization and for generating the statistics. Clustering coefficient (ranges from 0 to 1) measures the extent to which the nodes in the network tend to cluster together. Network centralization (ranges from 0 to 1) measures the extent to which the topology resembles a star. Network density (ranges from 0 to 1) shows how densely the nodes are connected in the network. Network heterogeneity shows the tendency of the network to contain hub nodes.

S20 Fig



S20 Fig. Cell type markers and their expressions in dot plot used to identify the ileal non-epithelial cells.

S21 Fig



S21 Fig. Cell type markers and their expressions in dot plot used to identify the ileal epithelial cells.